



The Pulvinar Regulates Information Transmission Between Cortical Areas Based on Attention Demands

Yuri B. Saalman *et al.*

Science **337**, 753 (2012);

DOI: 10.1126/science.1223082

This copy is for your personal, non-commercial use only.

If you wish to distribute this article to others, you can order high-quality copies for your colleagues, clients, or customers by [clicking here](#).

Permission to republish or repurpose articles or portions of articles can be obtained by following the guidelines [here](#).

The following resources related to this article are available online at www.sciencemag.org (this information is current as of October 10, 2013):

Updated information and services, including high-resolution figures, can be found in the online version of this article at:

<http://www.sciencemag.org/content/337/6095/753.full.html>

Supporting Online Material can be found at:

<http://www.sciencemag.org/content/suppl/2012/08/08/337.6095.753.DC1.html>

This article **cites 54 articles**, 19 of which can be accessed free:

<http://www.sciencemag.org/content/337/6095/753.full.html#ref-list-1>

This article has been **cited by** 6 articles hosted by HighWire Press; see:

<http://www.sciencemag.org/content/337/6095/753.full.html#related-urls>

This article appears in the following **subject collections**:

Neuroscience

<http://www.sciencemag.org/cgi/collection/neuroscience>

of dKO mice (Fig. 4C). dKO mice did not reveal BG process retractions at that stage (see above). However, 3 months after injections, when BG process retraction was evident, dKO mice displayed significant deficits in their motor performance when challenged on the Erasmus Ladder (Fig. 4D); they showed more missteps per trial. There were no signs of learning deficits, in that dKO mice improved their performance during the training sessions, similar to controls. When we subjected the animals at the same postinjection periods to the eyeblink conditioning paradigm, we observed that timing and amplitude of unconditioned responses (URs) of dKO mice (Fig. 4, E, F, H, and I), as well as rate of memory acquisition or extinction of conditioned responses, (figs. S15 and S16) were indistinguishable from controls. However, at 3 months posttreatment, the amplitudes of their conditioned responses (extent of eyelid closures) were significantly lower than those of controls after consecutive training sessions (Fig. 4J). Retraction of BG processes from PC synapses may impair timing of PC firing (with millisecond precision), which, in turn, would affect the output of cerebellar nuclei neurons and, thus, conditioned behavior (20, 21).

We addressed the role of BG AMPARs on cerebellar function by generating conditional

AMPA mutants where both GluA1 and GluA4 subunits were efficiently ablated in young and adult mice. We revealed that AMPAR signaling of BG cells contributes to the structural and functional integrity of the cerebellar network. Our results provide *in vivo* evidence that BG AMPARs play an important role in the fine-tuning of neuronal processing, which is crucial for a fast and precise control of complex motor behaviors.

References and Notes

1. A. Volterra, J. Meldolesi, *Nat. Rev. Neurosci.* **6**, 626 (2005).
2. A. Verkhratsky, F. Kirchhoff, *J. Anat.* **210**, 651 (2007).
3. G. Perea, M. Navarrete, A. Araque, *Trends Neurosci.* **32**, 421 (2009).
4. K. Matsui, C. E. Jahr, M. E. Rubio, *J. Neurosci.* **25**, 7538 (2005).
5. J. Grosche et al., *Nat. Neurosci.* **2**, 139 (1999).
6. M. Iino et al., *Science* **292**, 926 (2001).
7. T. Mori et al., *Glia* **54**, 21 (2006).
8. D. Zamanillo et al., *Science* **284**, 1805 (1999).
9. E. C. Fuchs et al., *Neuron* **53**, 591 (2007).
10. T. Müller, T. Möller, T. Berger, J. Schnitzer, H. Kettenmann, *Science* **256**, 1563 (1992).
11. N. Burnashev et al., *Science* **256**, 1566 (1992).
12. For more details, see supplementary materials on Science Online.
13. M. Lavialle et al., *Proc. Natl. Acad. Sci. U.S.A.* **108**, 12915 (2011).
14. H. Hirai et al., *Nat. Neurosci.* **8**, 1534 (2005).
15. E. M. Ullian, S. K. Saperstein, K. S. Christopherson, B. A. Barres, *Science* **291**, 657 (2001).

16. K. S. Christopherson et al., *Cell* **120**, 421 (2005).
17. R. S. Van Der Giessen et al., *Neuron* **58**, 599 (2008).
18. D. A. McCormick, R. F. Thompson, *Science* **223**, 296 (1984).
19. S. K. Koekkoek et al., *Science* **301**, 1736 (2003).
20. C. I. De Zeeuw et al., *Nat. Rev. Neurosci.* **12**, 327 (2011).
21. A. L. Person, I. M. Raman, *Nature* **481**, 502 (2012).

Acknowledgments: We thank K.-A. Nave for continuous support, S. Rudolph and P. G. Hirlinger for early contributions, T. Ruhwedel and F. Rhode for technical assistance, and D. Rhode and C. Casper for animal husbandry. This work was supported by the Max-Planck Society (INSERM-AMIGO, F.K.); Deutsche Forschungsgemeinschaft (DFG)—Research Center Molecular Physiology of the Brain (F.K.); DFG-SPP 1172 (F.K. and J.W.D.); DFG-SFB870 (M.G.); DFG-SFB894 (F.K.); DFG-Transregio TRR43 (F.K.); European Union (EU)—FP7-202167 NeuroGLIA (F.K.) and FP7-ITN-237956 Edu-Glia (F.K.); RO1-DC006881 (M.E.R.); the Research Initiative in Membrane Biology University of Kaiserslautern (J.W.D.); the Dutch Organization for Medical Sciences (C.I.D.Z.); Life Sciences (C.I.D.Z.); Fund for Economic Structure Reinforcement (NeuroBasic; C.I.D.Z.); Prinses Beatrix Fonds (C.I.D.Z.); and the EU ERCadvanced, CEREBNET, and C7 programs (C.I.D.Z.).

Supplementary Materials

www.sciencemag.org/cgi/content/full/science.1221140/DC1
Materials and Methods
Supplementary Text
Figs. S1 to S16
References (22–35)

27 February 2012; accepted 14 June 2012
Published online 5 July 2012;
10.1126/science.1221140

The Pulvinar Regulates Information Transmission Between Cortical Areas Based on Attention Demands

Yuri B. Saalmann,^{1,2*} Mark A. Pinsk,^{1,2†} Liang Wang,^{1,2†} Xin Li,^{1,2} Sabine Kastner^{1,2}

Selective attention mechanisms route behaviorally relevant information through large-scale cortical networks. Although evidence suggests that populations of cortical neurons synchronize their activity to preferentially transmit information about attentional priorities, it is unclear how cortical synchrony across a network is accomplished. Based on its anatomical connectivity with the cortex, we hypothesized that the pulvinar, a thalamic nucleus, regulates cortical synchrony. We mapped pulvino-cortical networks within the visual system, using diffusion tensor imaging, and simultaneously recorded spikes and field potentials from these interconnected network sites in monkeys performing a visuospatial attention task. The pulvinar synchronized activity between interconnected cortical areas according to attentional allocation, suggesting a critical role for the thalamus not only in attentional selection but more generally in regulating information transmission across the visual cortex.

The limited capacity of the visual system does not permit simultaneous processing of all information from our cluttered environment in detail. Selective attention helps overcome this limitation by preferentially routing behaviorally relevant information across the vi-

sual system. Simultaneous neural recordings from two cortical areas have suggested that this selective routing depends on the degree of synchrony between neuronal groups in each cortical area (1–4). However, it is unclear how different cortical areas synchronize their activity. Although direct interaction between two cortical areas may give rise to their synchrony, an alternative possibility is that a third area, connected to both of them, mediates cortical synchronization.

Higher-order thalamic nuclei, such as the pulvinar, predominantly receive input from the cortex rather than the periphery, and their output

strongly influences cortical activity in *in vitro* experiments (5). Because directly connected cortical areas are also indirectly connected via the pulvinar (fig. S1), the pulvinar is ideally positioned to synchronize activity across the visual cortex (6–8). However, little is known about the functional role of these cortico-pulvino-cortical loops. Selective attention modulates the magnitude of response of macaque pulvinar neurons (9, 10), and both humans and macaques with pulvinar lesions commonly have attentional deficits (11, 12). We therefore hypothesized that the pulvinar increases synchrony between sequential processing stages across the visual cortex during selective attention.

Information transmitted along the ventral visual cortical pathway is sequentially processed in interconnected areas V4 and the temporo-occipital area (TEO). We simultaneously recorded neural activity in macaques in the pulvinar, V4, and TEO during 51 recording sessions (13). Spike trains and local field potentials (LFPs) were recorded in each area from neurons with overlapping receptive fields (RFs). Monkeys performed a variant of the Eriksen flanker task, in which a spatial cue signals the location of a subsequent target flanked by distracter stimuli (target detection >80% accuracy overall; Fig. 1A). Because directly connected cortical areas such as V4 and TEO only connect with restricted but overlapping zones in the pulvinar (8, 14), we used diffusion tensor imaging (DTI) to ensure that electrodes targeted interconnected pulvino-cortical sites.

We performed probabilistic tractography on DTI data for each monkey to map probable

¹Princeton Neuroscience Institute, Princeton University, Princeton, NJ 08544, USA. ²Department of Psychology, Princeton University, Princeton, NJ 08544, USA.

*To whom correspondence should be addressed. E-mail: saalmann@princeton.edu

†These authors contributed equally to this work.

connections between the pulvinar, V4, and TEO. We identified pulvinar zones connected with V4 (yellow) and TEO (red) and delineated the region of overlap (green) that the V4-pulvinar-TEO pathway probably traverses (Fig. 1, B and C). V4 and TEO predominantly connected to the ventral pulvinar, and there was substantial overlap between V4 and TEO projection zones in the pulvinar, with the TEO projection zone extending more caudally, consistent with previous anatomical tracer work (8, 14). However, probabilistic tractography data had the advantage of delineating projection zones specific to individual monkeys, which cannot be precisely ascribed on the basis of published tracer data. Guided by our structural connectivity maps, we positioned electrodes in the appropriate projection zones and verified their location therein by taking structural scans of each electrode track (fig. S7). We performed additional tractography analyses between voxels containing electrode tips to show probable paths running directly between recording sites (Fig. 1, D to F).

If the pulvinar plays an important role in selective attention, then pulvinar neurons should signal where the monkey attends in our flanker task. Figure 2, A and B, show the population activity of pulvinar neurons aligned to the cue and target onsets, respectively. Pulvinar neurons responded robustly to the cue in their RF. While the monkey maintained attention at the RF location, there remained a small but significant increase in pulvinar activity across the delay period (Student's *t* test, $P < 0.05$). When a stimulus later appeared in the RF, pulvinar neurons showed a significantly greater response when the monkey attended to the RF location rather than outside the RF (in the opposite visual hemifield; *t* test, $P < 0.05$). These results are consistent with previously reported attention-enhanced pulvinar responses to visual stimuli (10), and they additionally show that the attentional locus is represented by the pulvinar spike rate throughout the delay period when no stimuli are present.

We further tested whether attention influenced pulvinar spike timing, specifically the synchrony between pulvinar neurons, by calculating the degree of synchrony between spike times and the LFP, or spike-field coherence. For spectral analyses, we largely focused on the delay period after the cue-evoked response until the array onset, because not only did the monkey maintain spatial attention during this interval, but the data in each session generally satisfied methodological assumptions of stationarity as well. Figure S2, A and B, show a typical session in which pulvinar spike-field coherence increased immediately after the cue appeared in the RF, predominantly in the alpha-frequency range. While the monkey attended to the RF location, the spike-field coherence remained significantly elevated throughout the delay period until target presentation (*t* test, $P < 0.05$). When the cue appeared outside the RF (fig. S2, C and D), drawing the monkey's attention away from the RF, there was much weaker

spike-field coherence. At the population level, there was significantly greater spike-field coherence in the 8- to 15-Hz range (alpha band) during the delay period, until target presentation when the monkey attended to the RF location rather than outside the RF (Holm's controlled *t* tests, $P < 0.05$; Fig. 2C). Because synchronized thalamic output provides increased drive to the cortex in anesthetized animals (15, 16), increased synchrony of pulvinar neurons may be an effective means to influence the visual cortex during selective attention.

We next aimed to establish that selective attention increased synchrony between cortical areas (1–3). We calculated the coherence between V4 and TEO LFPs, which measures the synchrony between oscillatory processes in the two areas, as a function of oscillation frequency. Attention generally increased coherence between V4 and TEO LFPs in two frequency bands. There was significantly increased mean coherence in the 8- to 15-Hz range, as well as a smaller but significant increase in the 30- to 60-Hz range (gamma band) across the population (Holm's controlled *t* tests, $P < 0.05$) during the delay period until target presentation (Fig. 3A).

Because low-frequency oscillations modulate higher-frequency oscillations (17–19), we tested

whether attention increased cross-frequency coupling between alpha and gamma oscillations within V4 and TEO. To measure cross-frequency coupling, we calculated the synchronization index between cortical alpha oscillations and the gamma power envelope. Across the population, there was a significantly greater synchronization index for V4 and TEO during the delay period, when attention was directed to the RF location rather than outside the RF (sign tests, $P < 0.05$; fig. S3, A and B), suggesting that alpha oscillations contributed to the attention effect on gamma frequencies.

If the pulvinar interacts with the cortex during attentional processing, then attention should also modulate pulvino-cortical synchrony. Across the population, there was significantly greater alpha-band coherence between the pulvinar LFP and V4 LFP (Fig. 3B), as well as between the pulvinar LFP and TEO LFP (Fig. 3C) during the delay period until target presentation, when the monkey attended to the RF location rather than outside the RF (Holm's controlled *t* tests, $P < 0.05$). This result is consistent with previous reports of synchrony between the cat lateral posterior-pulvinar complex and visual cortex (20, 21). Pulvinar spike trains also synchronized with cortical LFPs. Figure 3, D and E, respectively

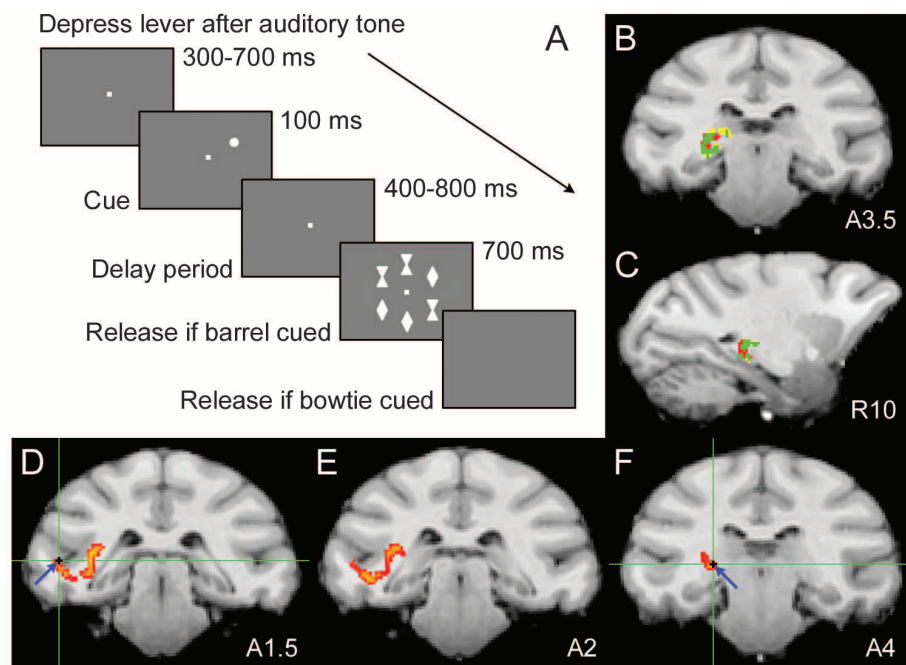


Fig. 1. DTI-defined pulvino-cortical network probed with spatial attention task. **(A)** We simultaneously recorded from the pulvinar, V4, and TEO of monkeys performing a flanker task. Monkeys maintained fixation throughout the trials while we manipulated their locus of attention. The monkeys' attention was drawn to the location of a cue, which randomly appeared at one of six locations. The cue signaled the location of the target in the subsequent array of six stimuli. To receive a juice reward, monkeys immediately released the lever after the onset of a barrel-shaped target or after the disappearance of the stimulus array for a bowtie-shaped target. **(B)** Coronal and **(C)** sagittal slices containing pulvinar voxels with a high probability of connection with V4 (yellow), TEO (red), or both (green). A3.5, 3.5 mm anterior to the interaural line; R10, 10 mm to the right of the midsagittal line. **(D to F)** Sequential coronal slices showing probable paths (yellow-red) between electrode tips [blue arrows and green cross-hairs in **(D)** and **(F)**] in TEO **(D)** and pulvinar **(F)** for one session.

show attention effects aligned to cue and target onsets for a typical session. Attention significantly increased coherence between pulvinar spikes and V4 LFP after the cue appeared in the RF until target presentation, predominantly in the 8- to 15-Hz range (t test, $P < 0.05$). There was much weaker coherence after the cue had drawn attention away from the RF (Fig. 3, F and G). We obtained similar attention effects on the co-

herence between pulvinar spikes and TEO LFP (fig. S4). Across the population, spatial attention significantly increased the coherence between pulvinar spikes and V4 LFP (Fig. 3H), as well as between pulvinar spikes and TEO LFP (Fig. 3I), predominantly in the 8- to 15-Hz range, throughout the delay period until target presentation (Holm's controlled t tests, $P < 0.05$). These findings support the idea that the pulvinar is part of

the brain's attention network (9, 12, 22–24) and that it uses the alpha band as a fundamental operating mode.

To determine the direction of pulvino-cortical interactions, we calculated the conditional Granger causality in the frequency domain for the connections between the pulvinar, V4, and TEO. Conditional Granger causality measures the influence that one area (e.g., the pulvinar) has on a second area (e.g., TEO), accounting for the influence of other areas (e.g., V4). This allowed us to dissect contributions from each connection and thus test our overall hypothesis that the pulvinar modulates cortical synchrony according to attentional demands. The pulvinar influenced oscillatory activity in both V4 and TEO when the monkey attended to the RF location. Figure 4, A and B, show that pulvinar influence on alpha activity in V4 significantly increased ($P < 0.05$) after the cue and continued until target presentation. There was much weaker pulvinar influence on V4 when the cue had drawn attention away from the RF (Fig. 4, C and D). Across the population, pulvinar influence on V4 (Fig. 4E; Holm's controlled t tests, $P < 0.05$) and on TEO (Fig. 4F; Holm's controlled t tests, $P < 0.05$) in the alpha-frequency range during the delay period was significantly greater with attention at the RF location than outside the RF. Pulvinar influence on alpha activity in both V4 and TEO correlated with the attentional modulation of synchrony between V4 and TEO in the same frequency range (Fig. 3A), suggesting that the pulvinar regulated alpha synchrony between cortical areas according to attention allocation.

In contrast to pulvino-cortical influences, direct cortico-cortical influences during the delay period were weak. Figure 4, G and H, show the population conditional Granger causality spectra for V4's influence on TEO and TEO's influence on V4, respectively. Spatial attention did not significantly change the weak influence of V4 on TEO, nor the weak influence of TEO on V4, during the delay period (t tests, $P > 0.05$). However, there was evidence consistent with strong cortico-cortical influences during visual stimulation (fig. S5). These results suggest that the maintenance of attention in the absence of visual stimulation depended on pulvino-cortical interactions (supplementary materials text) rather than direct cortico-cortical interactions.

Our results show that the pulvinar modulates the synchrony between cortical areas according to the locus of attention. The pulvinar predominantly influenced cortical alpha oscillations, consistent with another thalamic nucleus, the lateral geniculate nucleus, driving occipital alpha rhythms (25). Evidence suggests that the rhythmic excitability of alpha oscillations gates visual events, with the phase of alpha oscillations being critical for the transmission of visual information (26–28). Thus, the pulvinar, by synchronizing distributed patches of cortical alpha activity, can selectively facilitate transmission of information about attentional priorities across the cortex. Because pulvinar-

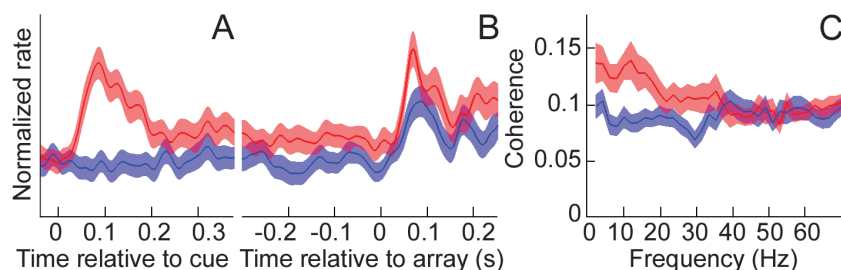


Fig. 2. Attention-modulated pulvinar spike rate and spike timing. Population activity (\pm SE) aligned to (A) cue and (B) target onset is shown as the mean of 51 pulvinar cells. In (B), the preferred stimulus (barrel or bowtie) appeared at the RF, flanked by congruent distracters. (C) Population average of the transformed spike-field coherence in the pulvinar, calculated in the 300-ms window before target onset. Red, attention at the RF; blue, attention away from the RF.

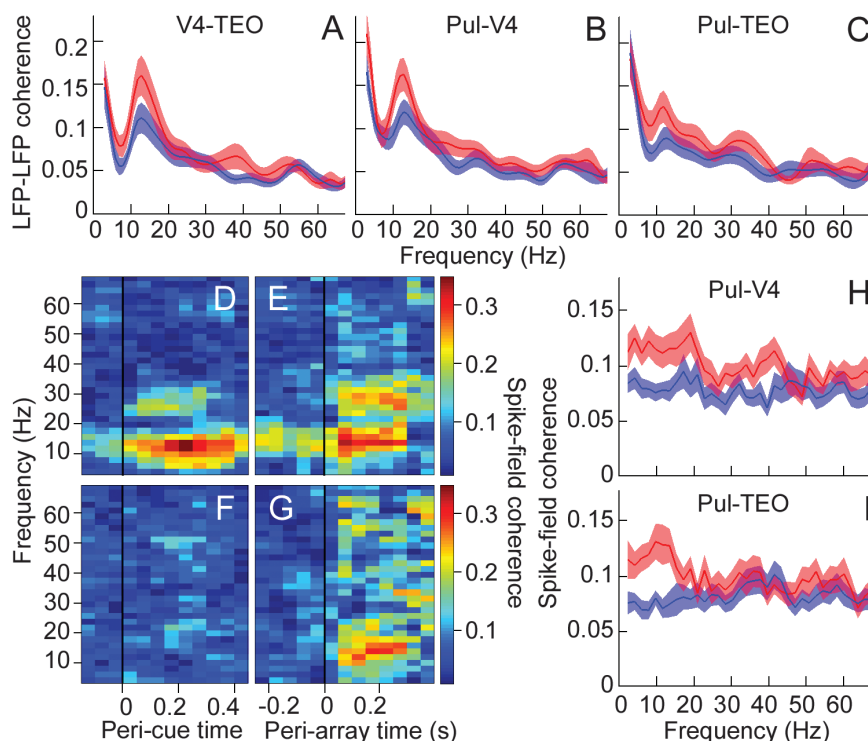
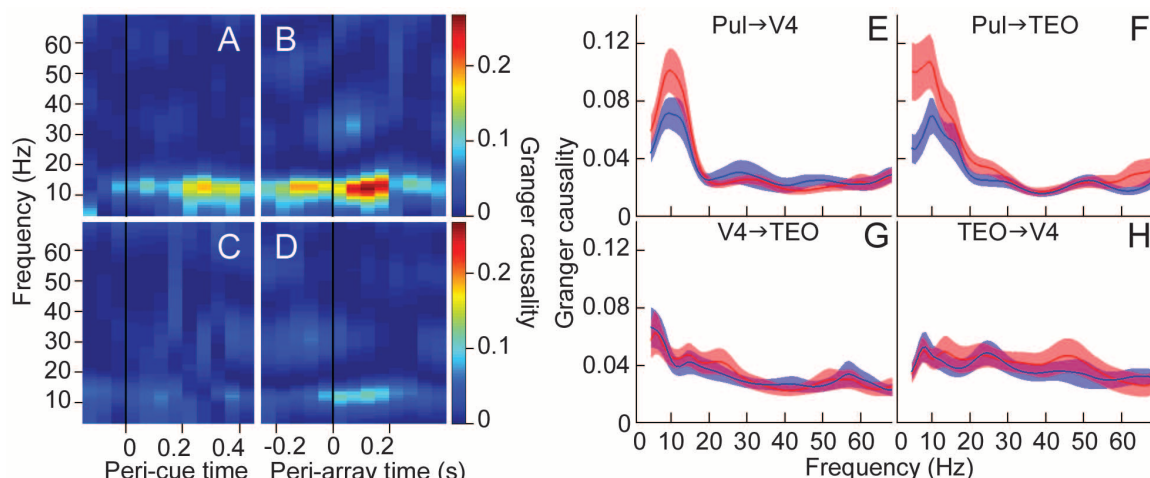


Fig. 3. Attention-modulated neural synchrony in pulvino-cortical networks. The population average of the transformed coherence between LFPs in (A) V4 and TEO, (B) pulvinar and V4, and (C) pulvinar and TEO, calculated in the 200-ms window before target onset, is shown. (D to G) Coherence (color-coded) between pulvinar spikes and V4 LFP for one session, calculated in successive 300-ms windows with a step size of 50 ms. (D) Cue and (E) target at the RF. (F) Cue and (G) target away from the RF. The same stimuli were presented in (E) and (G). The window immediately before the vertical black line in (E) and (G) represents the coherence 0 to 300 ms before target onset. The population average of the transformed coherence between (H) pulvinar spikes and V4 LFP and (I) pulvinar spikes and TEO LFP, calculated in the 300-ms window before target onset, is shown. Red, attention at the RF; blue, attention away from the RF.

Fig. 4. The pulvinar causally influenced cortical synchrony. (A to D) Conditional Granger causality (color-coded) from the pulvinar to V4 (accounting for TEO) for one session, calculated in successive 200-ms windows with a step size of 50 ms. (A) Cue and (B) target at the RF. (C) Cue and (D) target away from the RF. The same stimuli were presented in (B) and (D). The window immediately before the vertical black line in (B) and (D) represents the Granger causality 0 to 200 ms before target onset. The population average of the conditional Granger causality for (E) pulvinar influence on V4, (F) pulvinar influence on TEO, (G) V4 influence on TEO, and (H) TEO influence on V4, calculated in the 200-ms window before target onset, is shown. Red, attention at the RF; blue, attention away from the RF.



controlled alpha activity modulated gamma activity in the cortex through cross-frequency coupling, pulvinar influence on cortical synchrony extends to frequencies higher than the alpha frequency.

Pulvinar control of cortical processing challenges the common conceptualizing of cognitive functions as being restricted to the cortex. Pulvino-cortical influences dominated during the delay period, suggesting that internal processes such as the maintenance of attention in expectation of visual stimuli and short-term memory rely heavily on pulvino-cortical interactions. Pulvinar regulation of alpha activity is consistent with the important role ascribed to alpha oscillations in these internal processes (26, 29).

The prevailing view that information about our visual environment is transmitted through a network of cortical areas for detailed processing needs to be revised by considering extensive pulvino-cortical loops that regulate the information transmitted between each cortical stage of visual processing. Because of common cellular mechanisms and thalamo-cortical connectivity principles across sensorimotor domains, a general function of higher-order thalamic nuclei may be the regulation of cortical synchrony to selectively route information across the cortex.

References and Notes

1. T. J. Buschman, E. K. Miller, *Science* **315**, 1860 (2007).
2. G. G. Gregoriou, S. J. Gotts, H. Zhou, R. Desimone, *Science* **324**, 1207 (2009).
3. Y. B. Saalmann, I. N. Pigarev, T. R. Vidyasagar, *Science* **316**, 1612 (2007).
4. T. Womelsdorf *et al.*, *Science* **316**, 1609 (2007).
5. B. B. Theyel, D. A. Llano, S. M. Sherman, *Nat. Neurosci.* **13**, 84 (2010).
6. E. G. Jones, *Trends Neurosci.* **24**, 595 (2001).
7. Y. B. Saalmann, S. Kastner, *Neuron* **71**, 209 (2011).
8. S. Shipp, *Philos. Trans. R. Soc. London B Biol. Sci.* **358**, 1605 (2003).
9. D. B. Bender, M. Youakim, *J. Neurophysiol.* **85**, 219 (2001).
10. S. E. Petersen, D. L. Robinson, W. Keys, *J. Neurophysiol.* **54**, 867 (1985).
11. S. E. Petersen, D. L. Robinson, J. D. Morris, *Neuropsychologia* **25**, (1A), 97 (1987).
12. J. C. Snow, H. A. Allen, R. D. Rafal, G. W. Humphreys, *Proc. Natl. Acad. Sci. U.S.A.* **106**, 4054 (2009).
13. Materials and methods are available as supplementary materials on *Science Online*.
14. C. Baleyrier, A. Morel, *Vis. Neurosci.* **8**, 391 (1992).
15. J. M. Alonso, W. M. Usrey, R. C. Reid, *Nature* **383**, 815 (1996).
16. R. M. Bruno, B. Sakmann, *Science* **312**, 1622 (2006).
17. R. T. Canolty, R. T. Knight, *Trends Cogn. Sci.* **14**, 506 (2010).
18. O. Jensen, L. L. Colgin, *Trends Cogn. Sci.* **11**, 267 (2007).
19. C. E. Schroeder, P. Lakatos, *Trends Neurosci.* **32**, 9 (2009).
20. S. Molotchnikoff, S. Shumikhina, *Vision Res.* **36**, 2037 (1996).
21. A. Wróbel, A. Ghazaryan, M. Bekisz, W. Bogdan, J. Kamiński, *J. Neurosci.* **27**, 2230 (2007).
22. R. Desimone, M. Wessinger, L. Thomas, W. Schneider, *Cold Spring Harb. Symp. Quant. Biol.* **55**, 963 (1990).
23. D. LaBerge, M. S. Buchsbaum, *J. Neurosci.* **10**, 613 (1990).
24. D. L. Robinson, S. E. Petersen, *Trends Neurosci.* **15**, 127 (1992).
25. S. W. Hughes, V. Crunelli, *Neuroscientist* **11**, 357 (2005).
26. S. Palva, J. M. Palva, *Front. Psychol.* **2**, 204 (2011).
27. N. A. Busch, J. Dubois, R. VanRullen, *J. Neurosci.* **29**, 7869 (2009).
28. K. E. Mathewson, G. Gratton, M. Fabiani, D. M. Beck, T. Ro, *J. Neurosci.* **29**, 2725 (2009).
29. A. von Stein, C. Chiang, P. König, *Proc. Natl. Acad. Sci. U.S.A.* **97**, 14748 (2000).

Acknowledgments: We thank C. D. Brody and C. J. Honey for useful comments on the manuscript and M. Ding for Granger causality routines. Supported by NIH (grant R21 EY021078) and NSF (grant BCS-1025149).

Supplementary Materials

www.sciencemag.org/cgi/content/full/337/6095/753/DC1

Materials and Methods

Supplementary Text

Figs. S1 to S7

References (30–59)

9 April 2012; accepted 14 June 2012

10.1126/science.1223082